The Journal of Neuroscience, January 1993, 13(1): 127–143

Growth Cone Dynamics during the Migration of an Identified Commissural Growth Cone

Paul Z. Myers and Michael J. Bastiani

Department of Biology, University of Utah, Salt Lake City, Utah 84112

We have used time-lapse video microscopy to study the behavior of a neuron, Q1, that pioneers the posterior commissure of the embryonic grasshopper. Our goal is to use time-lapse video as a tool to acquire a precise picture of normal development over time, and thereby identify stereotypic activities that might indicate important interactions necessary for proper formation of the commissure.

We have identified specific and reproducible behaviors that suggest the presence of underlying cellular interactions that may play a role in pathfinding. In particular, the Q1 growth cone undergoes several morphological changes as it contacts the midline. As a commissural neuron, the midline may be a target in its outgrowth; Q1's typical response upon contacting the midline with its filopodia, however, is a rapid retraction. This inhibitory reaction can be overridden by contact with filopodia of its contralateral homolog. Q1's growth cone can translocate across the midline at an accelerated rate by a process resembling "filopodial dilation" (O'Connor et al., 1990) once the two Q1 growth cones meet. Ablation of the contralateral Q1 blocks Q1's advance across the midline.

We have also analyzed in detail the behavior of individual filopodia to identify behavioral differences that could indicate differences in substrate adhesivity. Except for instances of filopodial dilation seen only at the midline, we found no significant asymmetries in rates of filopodial extension and retraction, or in the survival times of individual filopodia. We suggest that either the adhesive signal used by Q1 is relatively weak, requiring the integration of many adhesive interactions by many filopodia to be resolved, or the guidance cues may not be adhesive in nature.

[Key words: growth cone, time-lapse video, commissure, grasshopper, pathfinding, filopodia, confocal microscopy, adhesion]

The migration of growth cones *in vivo* is a complex and dynamic process. We can infer this from even a cursory survey of growth cone illustrations in the literature; the elaborate and highly variable morphology of the growth cone suggests a rapidly changing structure with a complex architecture. When he first described them, Ramón y Cajal (1937) eloquently imagined that "it could be compared to a living battering ram, soft and flexible." Unfortunately, Ramón y Cajal and most researchers since that time have had to visualize the living growth cone on the basis of fixed, static material. An elegant exception to this limitation was first developed by Harrison (1907) and continued by Speidel (1933), who directly observed the extension of isolated nerve fibers *in vivo* and in tissue culture. Since that time, most of the observations of living growth cones have been made on isolated neurons in culture (Letourneau, 1979; Bray and Chapman, 1985; Smith, 1988). This valuable body of work has defined our ideas about the mechanics of growth cone migration. The typical growth cone radiates many fine processes called filopodia that rapidly extend and retract, and can contact substrates several tens of microns away; in addition, the growth cone can express ruffling, membranous veils or lamellae around its perimeter. However, the precise role of these structures is not clear. Filopodia, for instance, could be antennalike sensory structures, tension-generating "grappling hooks," or some combination of both.

One difficulty with much of the published work is that the growth cones are isolated and observed in artificially simple environments. Although simplifying the environment with tissue culture is a useful step toward identifying the basic mechanisms of growth cone movement, it also removes the extrinsic information needed for proper growth cone navigation. In recent years, advances in technology have made it possible to observe the living growth cone *in situ* (Myers et al., 1986; Harris et al., 1987; O'Rourke and Fraser, 1989; Godement et al., 1990; O'Connor et al., 1990) and so integrate a detailed dynamic study of growth cone behavior with an analysis of its extracellular environment during normal pathfinding.

The goal of this work is to observe the fine-scaled behavior of a growth cone *in vivo,* and from those observations infer the nature of any local interactions. Specifically, one class of behaviors that can be identified using these techniques is responses to regions of differential adhesivity. Growth cones can recognize and select between substrates with different adhesivities (Hammarback et al., 1985; Burmeister and Goldberg, 1988), their behavior can be regulated by mechanical tension (Zheng et al., 1991), and they in turn can exert mechanical force on other cells in their environment (Heidemann et al., 1990). Although the generation of mechanical force cannot be assayed by the techniques used in this article, other indirect responses of the growth cone to changes in adhesion should be visible: changes in growth cone shape and rates of migration, filopodial stabilization, and more subtle variations in the rate of filopodial extension and retraction. Because the growth cone is navigating in a well understood embryonic environment (Taghert et al., 1982), we can also correlate filopodial behaviors with contacts with putative guidepost cells.

Additional nonadhesive mechanisms of cell–cell communication have been reported in the literature that are also detect-

Received Oct. 25, 1991; revised July 13, 1992; accepted July 15, 1992.

We thank Rommy von Bernhardi, Ellen Carpenter, Rolf Karlstrom, and Elaine Seaver for their discussion and helpful criticism of the manuscript. This work was supported by 5T32 CA09602 and NS08656 to P.Z.M. and NS25378 and a McKnight Foundation award to M.J.B.

Correspondence should be addressed to Dr. Paul Z. Myers at the above address.

able by time-lapse microscopy. Cultured neurons grown in the presence of other, presumably incompatible, neurons can exhibit growth cone inhibition (Kapfhammer and Raper, 1987; Raper and Kapfhammer, 1990), and the phenomenon has also been observed *in situ* (Godement et al., 1990). Growth cone inhibition is a rapid, discrete behavior that can be triggered by a single filopodial contact; it is obviously nonadhesive in that it is a response that immediately prevents any kind of local interaction between two cells.

Not all interactions between cells will produce sufficiently rapid, discrete responses in the growth cone that can be resolved with time-lapse microscopy. For example, vertebrate commissural neurons can be induced to extend toward isolated floorplate explants (Tessier-Lavigne et al., 1988), suggesting that their growth cones may be following a gradient of an unidentified diffusible molecule. Retinal growth cones appear to recognize a gradient of an unidentified factor expressed on the tectal surface that has a slope of roughly 1% difference in concentration across the width of a growth cone (Baier and Bonhoeffer, 1992). Under such circumstances, the morphological effect on the growth cone by shallow gradients of adhesion or diffusible factors would be too subtle to be easily detectable.

Our time-lapse observations of the development of Q1 have revealed instances of obvious, discrete responses to contacts by filopodia that lead to specific behaviors by the growth cone, and instances in which growth cones make pathfinding decisions in the absence of any recognizable response by the filopodia. The results suggest that the growth cone may navigate to the midline by following either (1) a shallow gradient that is undetectable to our procedures or (2) a discrete cue that provides a nonadhesive signal that does not affect filopodial behavior. Progress beyond the midline is mediated by interaction with filopodia from a specific growth cone that bridge the midline.

Materials and Methods

DiI injections. We obtained grasshopper embryos, *Schistocerca americana,* from a colony maintained at the University of Utah. We dissected embryos from their eggs in a dish of culture medium, and staged them according to the criteria of Bentley et al. (1979). The medium consisted of 1.33% glycine dissolved in a solution of 55.6% Schneider's *Drosophila* medium (GIBCO) and 44.4% minimum essential medium (MEM) (GIBCO), with 0.001 μg/ml of juvenile hormone (Sigma) and 0.001 μg/ml of β-ecdysterone added. We then pinned embryos dorsal side up on a slide in a drop of medium, placed them on a Zeiss standard microscope, and observed them with a Leitz 50× water immersion lens and Nomarski optics. Individual neurons were labeled with glass microelectrodes drawn on a Sutter model P-80 puller and filled with 0.1–0.5% solution of 1,1′-dioctadecyl-3,3,3′,3′-tetramethylindocarbocyanine perchlorate (DiI; Molecular Probes) in 100% ethanol or dimethyl sulfoxide (DMSO) (Honig and Hume, 1986). A continuous, small (<0.5 nA) depolarizing current was used to generate a very slow, controlled flow of dye from the electrode tip; the electrode was then placed immediately adjacent to the cell of interest, and held in place for roughly one minute or until a barely observable quantity of dye had diffused over the surface of the soma. Care was taken to avoid actually penetrating the cell with the electrode tip.

Ablations. We killed cells by making an intracellular penetration with a Lucifer yellow–filled electrode and applying a large (±10 nA) alternating current as described by Myers and Bastiani (1992). Both the Q1 and Q2 neurons on one side of a ganglion were killed prior to 32% of development. We then cultured embryos for 24 hr, and assayed the growth of the surviving Q1 neuron on the other side of the ganglion either by intracellular injection of Lucifer yellow or by the extracellular application of DiI.

Embryo explant culture. After labeling a cell with DiI, or after ablating selected neurons, we unpinned the embryo and transferred it to fresh medium. The anterior and posterior portions of the embryo were cut away and discarded, and the central segments containing the labeled cell were pinned dorsal side down within a small well cut in a Sylgard-coated coverslip. An older embryo at greater than 60% of development, intact but for a small puncture at the posterior end to permit circulation of hemolymph into the medium, was cultured in the same well. We then inverted the coverslip and sealed it with Vaseline to a Sylgard-coated slide with a larger well cut in its surface. The slide and coverslip together formed a small chamber. In addition to the drop of medium containing the labeled embryo and cocultured older embryo, the chamber also contained two small drops of water to maintain humidity and a small hole, sealed with cotton and halocarbon oil, to allow limited passage of air. Embryos could live and grow healthily for several days in these chambered slides.

Time-lapse microscopy. Embryos within chambered slides were transferred to a Leitz Laborlux microscope in a room maintained at a temperature of approximately 30°C. We observed cells through either a 40× or 63× oil-immersion lens and illuminated with a 100 W halogen light filtered through the Leitz N2 (rhodamine) filter set, and shuttered with a computer-controlled Uniblitz shutter (Vincent Associates). Labeled cells were imaged with a B.F. Meyers MCP intensifier (Dark Invader) and Pulnix TM-740 CCD camera. A QuickCapture video digitizer (Data Translation, Inc.) installed in a Macintosh II computer digitized the video images. We processed the digitized images (typically with only some contrast and edge enhancement) using custom software called AXOVIDEO (Axon Instruments; Myers and Bastiani, 1991) and stored them on a Panasonic Optical Memory Disk Recorder (OMDR). Figures were produced by printing the images at two to four times the size of the digitized image on an Apple Laserwriter, and photographically reducing the resultant oversized image.

The AXOVIDEO software was designed both to regulate precisely the timing of image capture and to minimize exposure of the cells to illumination by controlling a shutter. We programmed the software to average two to four video frames every 1–5 min; most of our measurements were made on samples taken every 3 min. At these exposure rates, we found that DiI-labeled cells could grow at a steady and apparently healthy rate for 12–24 hr before showing obvious ill effects (retraction of filopodia, and sustained reduction in rate of extension). We found two factors that limited the viability of labeled cells: (1) simple mechanical damage during the injection procedure resulted in rapid and obvious death of the cells shortly after beginning observations, and (2) the introduction of too much dye into the cell membrane yielded cells that, although appearing healthy with active filopodia, were unable to maintain migration of their growth cone. The latter instance seemed to be a consequence of the cytotoxic effects of illuminating the cells, since growth could resume by subsequently culturing the embryo in the dark. Neurons that exhibited any of these symptoms were not used in any of the analyses presented in this article.

Filopodial measurements. We measured filopodia by selecting an arbitrary video frame of a growth cone at a particular stage of development, and tracking backward and forward through the video recording to follow the complete temporal sequence for all of the filopodia visible in that frame. This procedure produced a representative sample of all visible filopodia, unbiased by selection by the observer. We measured the orientation and length of each filopodium using manual tracing tools available in the AXOVIDEO software. We therefore made multiple measurements of the instantaneous rates of extension and retraction for each filopodium. Filopodia that increased in length between one measurement and the next were scored for extension rate, and filopodia that decreased were scored for retraction rate. Filopodia that were stable between one measurement and the next were scored as having an extension rate of 0 μm/hr; filopodia that were selectively stabilized would be readily apparent in the statistics by a greatly reduced average extension rate.

Although we attempted to make a complete sample of all the filopodia present at a particular instant, we could not accurately observe short filopodia that were medially oriented, since they tended to be obscured by their densely packed fluorescent neighbors. The data are therefore slightly biased by the resolution of our system to show fewer filopodia extending medially than are actually present, and the average length and duration of the medial population are calculated in the absence of this obscured population of shorter filopodia. The effect of this bias is to reduce the average calculated length and duration of laterally directed versus medially directed filopodia. We have attempted to compensate for this effect by also computing the statistics on only the longest 40% of the filopodia, in effect arbitrarily eliminating the shorter, laterally

Table 1. Filopodium parameters

	Mean value	Mean vector		D_n
		Angle	Magnitude	
32%				
n (129)	—	14.7°	0.52	—
Duration	36.5 ± 15.6 min	12.7°	0.18	**0.07, $p < 0.05$**
Peak length	21.2 ± 7.7 μm	0.2°	0.19	**0.07, $p < 0.05$**
Extension rate	88.3 ± 43.4 μm/hr	23.0	0.10	0.01, $p > 0.1$
Retraction rate	98.3 ± 38.7 μm/hr	5.7°	0.14	0.02, $p > 0.1$
32%, longest-lived 40%				
n (51)	—	−0.1°	0.65	—
Duration	52.4 ± 15.2 min	13.3°	0.27	<0.01, $p > 0.1$
Peak length	25.7 ± 7.5 μm	1.9°	0.28	0.02, $p > 0.1$
Extension rate	72.2 ± 30.1 μm/hr	1.8°	0.27	0.01, $p > 0.1$
Retraction rate	91.8 ± 41.8 μm/hr	11.4	0.29	0.05, $p > 0.1$
32.5%				
n (57)	—	25.3°	0.53	—
Duration	35.3 ± 17.7 min	5.8°	0.25	**0.16, $p < 0.01$**
Peak length	20.7 ± 7.1 μm	0.5°	0.22	0.08, $p > 0.1$
Extension rate	100.7 ± 62.2 μm/hr	28.1°	0.15	0.04, $p > 0.1$
Retraction rate	104.2 ± 40.4 μm/hr	23.1°	0.14	0.01, $p > 0.1$

Five parameters (number of filopodia, duration, length, and the extension and retraction rates) were measured for growth cones at two different times in development. At 32%, the Q1 growth cone is in the process of making a turn; at 32.5%, it has completed the turn and is growing to the midline. Because short-lived medially directed filopodia are obscured by the large numbers of medial filopodia, we have attempted to correct this bias in the sample by also examining a subset of the 32% filopodia, the longest-lived 40%. For each parameter, the mean value ± SD and the vector sum are given. An angle of 0° for the vector sum is medial; 90° is rostral; and 180° is lateral. The magnitude of the vector sum has been normalized to a range of 0.0–1.0. These two numbers quantify the magnitude and direction of any skewedness in the distribution of the parameter. For example, at 32% of development, the mean vector for filopodial duration has a magnitude of 0.18 and angle of 12.7°. This means that long-lived filopodia tend to cluster to a small extent in a particular orientation, 12.7°, which is slightly rostrally and medially. D_n is the circular–linear correlation coefficient determined by a ranked circular–linear correlation as described by Mardia (1976). This value is a measure of the deviation from a random distribution. Parameters that have a significantly skewed distribution have their p values displayed in boldface. The only parameters of filopodial behavior found to be statistically significant in their variation from a random distribution are duration and length at 32% of development, and duration alone at 32.5%. The distribution of filopodia at all time points is unambiguously skewed as determined by the Rayleigh test ($p < 0.001$), with many more filopodia extending medially. However, this skewed distribution does not arise by a selection mechanism, which would be apparent by a similarly strongly skewed distribution in the duration of individual filopodia. Although there is a small, statistically significant increase in the length of survival of medially directed filopodia, the difference disappears if only long-lived filopodia are examined, eliminating an experimental flaw in our sampling method. Equally long-lived filopodia are found on both the medial and lateral sides of the growth cone; the enhanced visibility of short filopodia on the sparsely populated lateral side reduces the mean duration of laterally directed filopodia.

directed filopodia (Table 1). Reducing our sample bias in this way results in the disappearance of any significant orientation preference by the filopodia. Since the conclusion of our analysis of the complete data set is that the filopodial orientation preferences are too small to account for the behavior of the growth cone, and the effect of flaws in the data set is to increase any observed orientation preference, the bias in our sample clearly has no substantial effect on our conclusions.

We tested the distribution of filopodia to determine whether it differed significantly from randomness by the Rayleigh test (Batschelet, 1981). A circular–linear correlation coefficient (D_n) for the parameters of filopodial behavior was determined using a ranked linear–circular correlation (Mardia, 1976; Batschelet, 1981).

Results

Reliability of the time-lapse procedure

We had two main questions about the utility of a time-lapse study: would the spatial resolution be adequate to observe the delicate structure of the growth cone? And, when observed with adequate resolution, would the behavior of the growth cone be sufficiently unaffected by the illumination that the observations would have some validity?

We answered the first question by comparing images captured by the time-lapse equipment at the same settings as would be used during a time-lapse experiment, with images of the same cell captured with a confocal microscope 20 min later (Fig. 1). Although it is clear that we cannot resolve all of the filopodia present (in particular, short filopodia adjacent to the bright neurite or growth cone are lost) and that there is a glaringly obvious difference in the crispness of the two images, we are confident that we can detect the orientation and extent of major filopodia. In addition, we have found that the temporal integration done by our eyes during the course of a playback greatly enhances the apparent resolution in a way that cannot be demonstrated in a still photograph.

In answer to our second concern about the invasiveness of the procedure, we have chosen as the subject of this time-lapse study the development of the commissural neuron Q1 (Fig. 2). We have studied and described the normal development of Q1 in detail (Myers and Bastiani, 1992) and therefore have a solid baseline of data obtained by more conventional means with which to compare the results of the time-lapse observations. We have found that the morphology of the growth cone is qualitatively similar in both fixed material and in cells subjected to time-lapse microscopy. Q1 has made only appropriate pathway

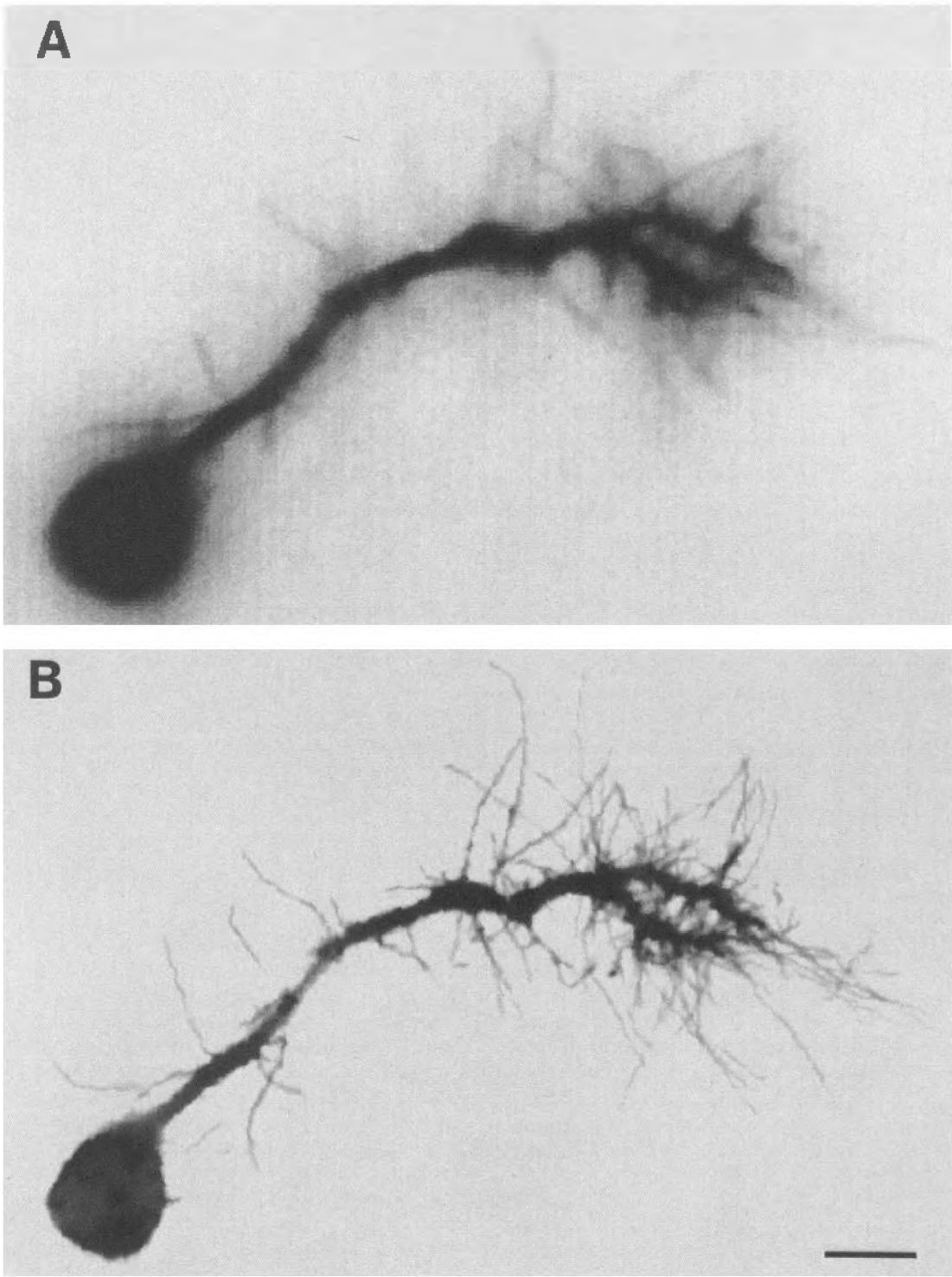

Figure 1. A comparison of the spatial resolution of the time-lapse video system with the Bio-Rad confocal microscope. Although resolution must be compromised to keep fluorescently labeled cells alive for an extended period, the system retains sufficient resolution to observe individual filopodia. *A*, An image digitized at a level of illumination comparable to that used in a typical time-lapse series, using a low level of shuttered illumination and an image intensifier and CCD camera. The level of illumination was comparable to what we would use in a time-lapse experiment that we intended to maintain for 24 hr or more. This image is the result of a four-frame average and some edge enhancement with a 3 × 3 convolution kernel. *B*, The same cell visualized 20 min later on a Bio-Rad MRC-600 confocal microscope. Some of the differences between *A* and *B* are a consequence of this difference in time. A high level of illumination was used to maximize resolution without regard for photo-damage to the cell. This image is a composite, built from a four-plane through-focus series, each plane separated by 2.5 μm and captured as a 16-frame average. The resulting image has also been enhanced with the same 3 × 3 sharpening convolution kernel as *A*. Scale bar, 10 μm.

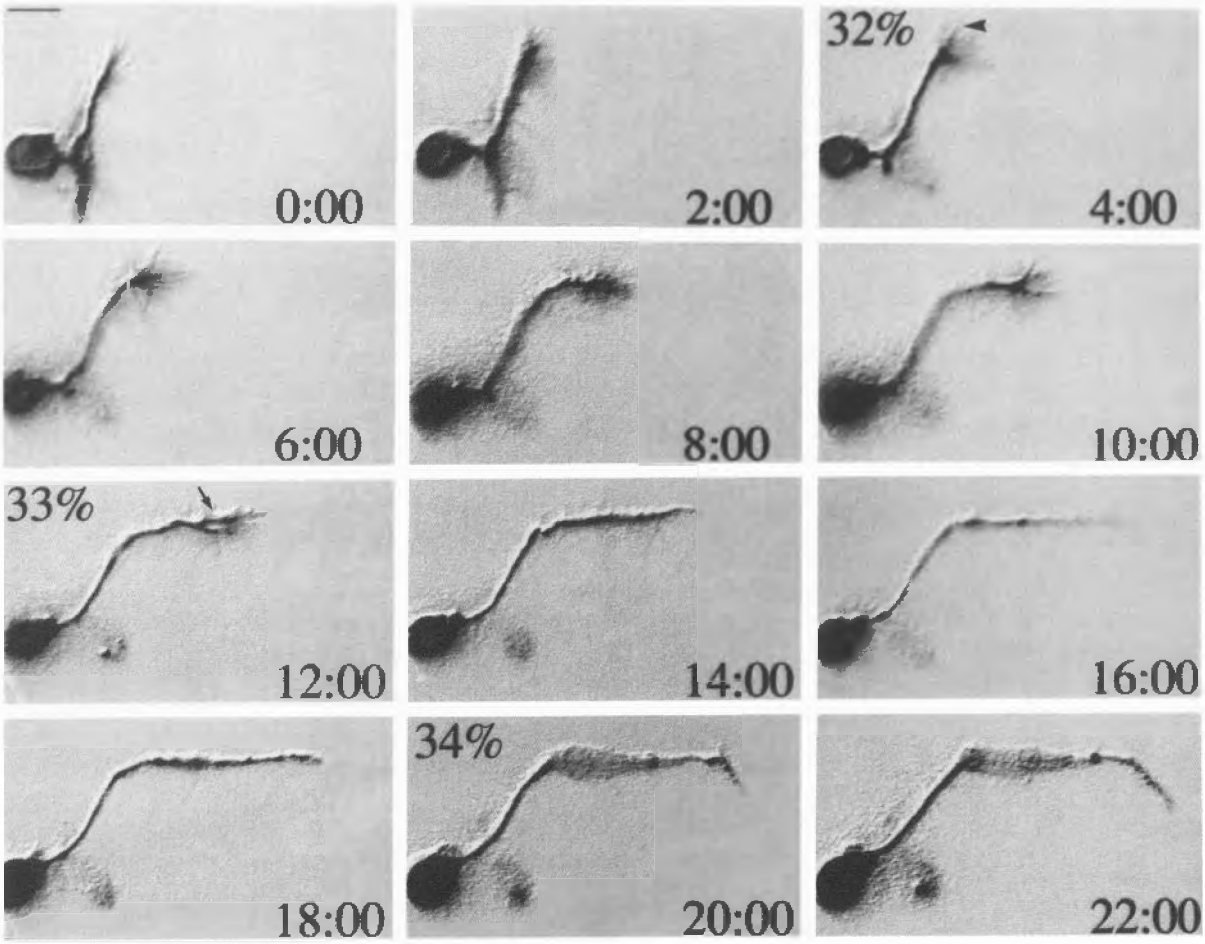

Figure 2. The Q1 growth cone follows a stereotyped pattern of migration. This series was recorded at a frequency of one frame every 3 min; a subset of those frames, one every 2 hr, is shown here. The recording was made at relatively low levels of illumination to permit a prolonged series, so not all filopodia are detectable, although the overall progress of the growth cone can be followed. The initial projection, between 30.5% and 32% of development (0–2 hr), is rostral, following the longitudinal fascicle pioneered by the MP1 and dMP2 neurons (not shown). The growth cone turns medially upon reaching the longitudinal level of the MP1 soma (4–6 hr), and extends over the MP1 soma (6–8 hr) and then to the midline (8–12 hr). In this example, the Q1 growth cone initially contacted the midline at shortly after 8 hr, but does not successfully cross it until about 11 hr. At the midline, the growth cone contacts the growth cone of the contralateral Q1 and fasciculates with its axon. The subsequent migration of the Q1 growth cone is first on the axon of the contralateral Q1 (14–18 hr), which it follows to the contralateral longitudinal fascicle (20–22 hr), where it switches substrates to grow caudally on the contralateral MP1 axon. Scale bar, 10 μm.

decisions while observed; there have been no gross aberrations in overall morphology. The rates of growth cone migration as measured during time-lapse microscopy have been consistently slower but still comparable to those calculated from timed incubations of embryos and measurements of fixed axon lengths. We estimate that the mean rate of Q1 growth cone extension in an undisturbed embryo is approximately 8 μm/hr; the directly measured mean rate over a comparable period of time in the time-lapse experiments is 4.2 μm/hr. The consistent difference in rates may be due to a difference in incubation temperature, since the time-lapse experiments were carried out in a less precisely controlled thermal environment. It is also possible, however, that some of the reduction in growth rates may be a direct consequence of DiI labeling; carbocyanine dyes can inhibit cellular metabolism (Terasaki, 1989). This reduction in growth cone migration rate was not accompanied by any obvious effect on pathfinding. None of the labeled neurons observed with time-lapse video microscopy displayed any significant variations from the morphology observed in static images of fixed embryos.

We also observed two clearly artifactual kinds of growth cone behavior. In a few cases (3 of 15), the Q1 growth cone showed signs of initial impairment in that it engaged in repeated cycles of extension and retraction that resulted in no net growth or reduced growth over a period of 2–4 hr (Fig. 3, asterisks). In all instances, this growth cone delay was observed immediately after injection and mounting, and is presumed to result from some insult dealt during preparation for the time lapse. In all three instances, the growth cone eventually recovered and resumed normal growth. Measurements from these cells made after their apparent recovery are included in the data set presented here. Not included in the data set are an additional three cases in which the initial trauma was more severe. In these three cases, Q1 appeared healthy in that it maintained an actively extending and retracting set of filopodia, but no growth cone extension occurred over a period between 10 and 20 hr. Although experimentally induced artifacts are not often desirable, this pattern of behavior is at least easily recognizable and, as a method for either delaying or halting axon growth, suggests a number of possible future experiments. Furthermore, the behavior of the filopodia appeared superficially indistinguishable

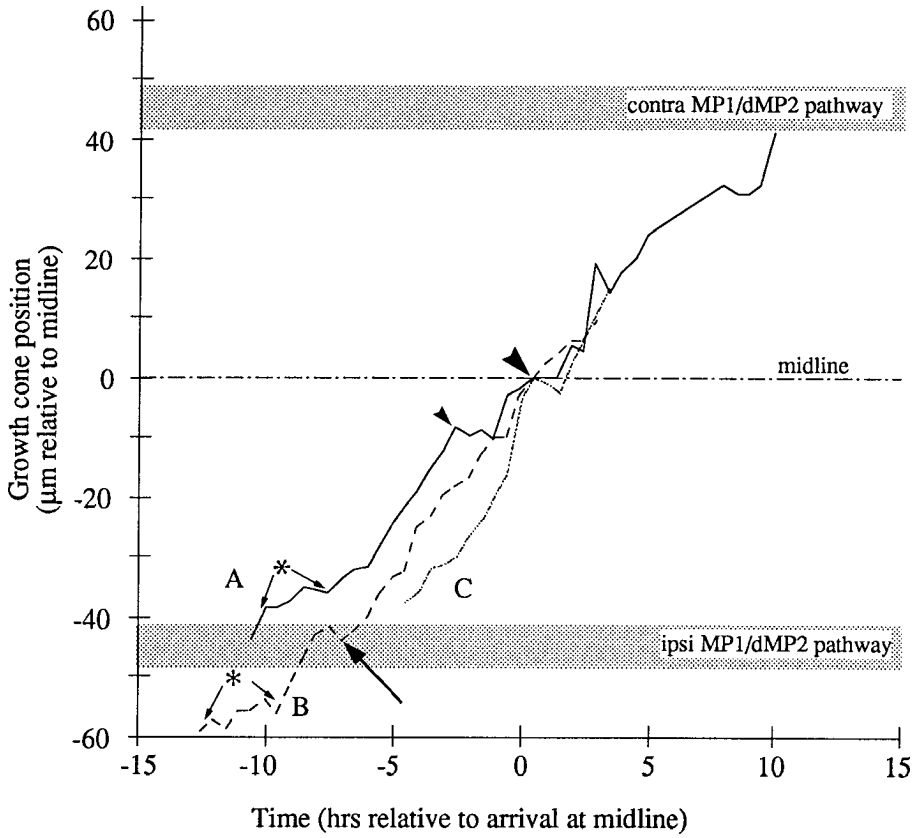

Figure 3. The distance of Q1's growth cone from the midline is plotted here as a function of time. Three representative traces have been aligned on the time at which they initially contact the midline. The midline is marked as a fine *broken line*; the approximate positions of the longitudinal MP1/dMP2 fascicles are marked with *broad gray stripes*. The Q1 growth cone initially migrates rostrally along the ipsilateral MP pathway; it then turns medially and extends to the midline, where it contacts the contralateral Q1 growth cone, fasciculates with it, and grows to the contralateral MP pathway. The progress of the growth cone is not smooth, but is interspersed with pauses, retractions, and bursts of forward growth. Most of these inconstancies in growth are not reproducible from cell to cell, but several characteristic behaviors are illustrated here. Specifically, growth cones extended too far rostrally and retracted before turning medially (*single arrow*), and retracted or paused within 20 μm of the midline (*small arrowhead*) or at the midline (*large arrowhead*). Several growth cones also exhibited an initial period of poor growth (*asterisks with arrows*) that we believe was artifactual. *A*, This growth cone was followed from the time it left the ipsilateral MP1/dMP2 pathway until it had just begun to turn caudally on the contralateral MP1/dMP2 pathway. The initial rate of growth was low (*asterisks*); this was most likely an artifact, as several growth cones exhibited a prolonged (2–4 hr) period of poor growth immediately after being injected with dye. The growth cone retracted 10 μm before reaching the midline (*small arrowhead*), at a time when its filopodia were extending across the midline. It also stopped all progress for 1 hr at the midline (*large arrowhead*). *B*, This growth cone was observed from shortly after axogenesis until the growth cone had progressed approximately 10 μm beyond the midline. It too exhibited an initial period of limited growth (*asterisk*) that is presumed to be a response to the injection procedure. The brief retraction as the growth cone crossed the ipsilateral MP1/dMP2 pathway (*single arrow*) was caused by an overshoot; the growth cone extended approximately 5 μm too far rostrally, then retracted and turned medially. The growth cone exhibited no notable behavior at the midline, progressing across it with no hesitation. Of the growth cones we observed, 47% showed no detectable changes in behavior as they crossed the midline. *C*, This growth cone extended rapidly and smoothly to the midline (*large arrowhead*), where it abruptly retracted. After being set back about 4 μm, it continued its growth. We observed that 53% of the growth cones either retracted or stopped (as did growth cone *A*) at the midline.

from that of filopodia in normally advancing growth cones, suggesting that growth cone migration is not a simple consequence of filopodial movements.

One final and easily discountable artifact was the eventual deterioration of the preparation after 1–2 d of growth. The transition from a healthy growth cone to a dead or dying one was typically sharp; filopodia retracted, the growth cone became club shaped, and migration either stopped entirely or was reduced to a fraction of a micrometer per hour.

Q1 outgrowth

We have documented the pattern of outgrowth of the Q1 neuron in the preceding companion article (Myers and Bastiani, 1992); we will briefly review it here (Fig. 2). Q1 is a neuron that arises early in the development of the embryonic nervous system and pioneers the posterior commissure. Q1 begins axon outgrowth at 31% of development, and initially extends a rostrally directed process that follows the longitudinal MP1/dMP2 fascicle (Fig. 2, 0–2 hr). At this time the Q1 growth cone contacts and becomes dye coupled with a pair of neurons, anterior and posterior corner cells (aCC and pCC), that lie medially to the Q1 soma and are also extending growth cones along the longitudinal fascicle contemporaneously with Q1. The Q1 growth cone turns medially, toward the MP1 soma at 32% of development and extends farther medially to reach the midline by 33% (Fig. 2, 4–12 hr). At the midline, the growth cone contacts the contralateral Q1 axon, which it follows to reach the contralateral longitudinal fascicle, where it turns to follow the contralateral MP1/dMP2 fascicle caudally (Fig. 2, 14–22 hr).

Although the spatial pattern of axon outgrowth in the grasshopper is stereotyped and precise, the temporal pattern appears much more erratic. Growth cone migration is not smooth and

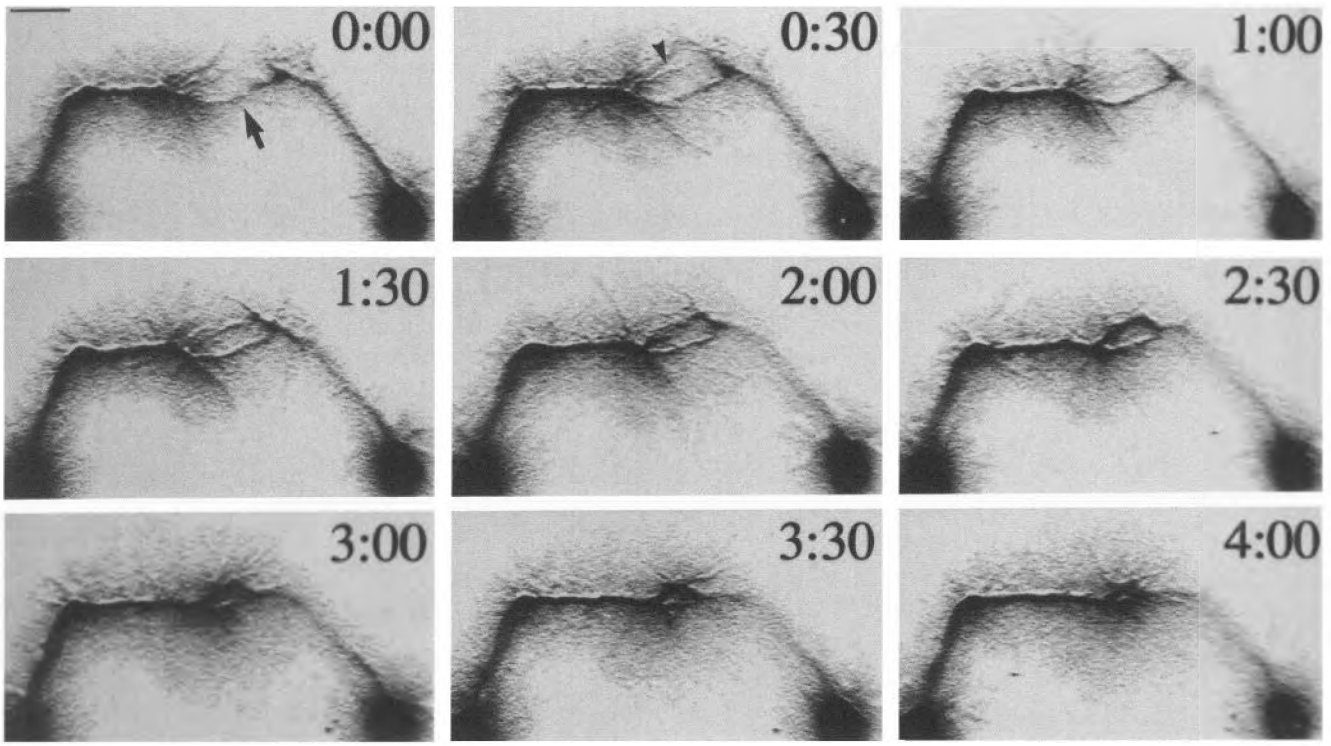

Figure 4. The Q1 growth cone exhibits a strong affinity for filopodia of its contralateral homolog. In this time series, both Q1 neurons in a single element were labeled with DiI (the neuron on the right was more lightly labeled) and observed as the growth cones converged on each other and the midline. The images were sampled at a rate of one frame every 3 min; the subset of frames reproduced here is separated by an interval of 30 min. The growth cones first contact each other via a pair of filopodia at time 0:00 (*arrow*), and a second pair make contact by time 0:30 (*arrowhead*). These filopodia are then stabilized and thicken, persisting for over 4 hr before they become totally subsumed into the advancing growth cone (time *4:00*). Note the initial misalignment of the two growth cones brought into linearity by the convergence on the filopodia at the point of contact. Scale bar, 25 μm.

continuous, but is marked by frequent pauses or short retractions that last for an hour or more, followed by brief bursts of growth at rates up to 25 μm/hr (Fig. 3). There is some variation in the time at which the Q1 growth cone reaches the midline, ±2 hr or ±0.4% of development, from animal to animal as measured from the time the growth cone makes its initial medial turn to the time it reaches the midline. This difference is comparable to that measured in fixed preparations. The pair of Q1 neurons in a single unperturbed segment typically vary by ±1.5 hr or ±0.3% of development from one another (P. Z. Myers and M. J. Bastiani, unpublished observations).

Although the cell-to-cell variability is a prominent feature of the temporal pattern of growth cone migration, we have also identified three common patterns of behavior by the Q1 growth cone: (1) a 10–15 μm overshoot past the appropriate turning point when Q1 should be making its initial medial turn, (2) an elaboration of the growth cone as it contacts the MP1 soma, and (3) either a retraction or a rapid translocation across the midline.

All of the Q1 growth cones observed from a time before making their medial turn to the midline ($n = 5$) exhibited an initial overshoot followed by a retraction (Figs. 2, arrowhead at 4 hr; 3, large arrowhead). The medial turn was not made by turning the growth cone, but by making a medial branch that was typically located 10–15 μm caudal to the leading edge of the growth cone. In four of the five cases, the medial branch appeared 30–60 min after the growth cone had extended beyond the turning point; in the remaining instance, the growth cone bifurcated to extend medially and rostrally simultaneously. In all cases, the rostral branch was retracted 2–3 hr after the appropriate medial branch had established itself.

In 7 of the 13 cases in which we observed the Q1 growth cone from the time of its medial turn to the time it reached the midline, we saw characteristic, transient changes in its morphology at the time it contacted the MP1 soma. These changes correspond with the changes we have observed with low frequency in fixed material (Myers and Bastiani, 1991). Most often (71%), the Q1 growth cone bifurcated, expressing a transient rostromedial branch that extended over the MP1 soma and beyond (Figs. 1; 2, arrow at 12 hr). This branch may be one source of the variation in growth rates: while the branch was extending, the main growth cone typically halted its migration, and resumed growth when the branch stopped or retracted. In two instances, the Q1 growth cone did not branch but instead broadened and flattened, presumably over the MP1 soma.

At the midline, the Q1 growth cone exhibited one of two distinctive behaviors. In eight of 15 instances, the growth cone stopped or abruptly retracted within 20 μm of the midline after one or more of its filopodia had reached the midline (Fig. 3, arrowheads). This delay persisted for 30–60 min, and in three cases, the growth cone repeated the retraction a second time after resuming growth and contacting the midline once again. Retraction of the growth cone did not necessitate withdrawal of filopodia from the midline, however, and the halted growth cones continued to extend filopodia actively to the midline and beyond.

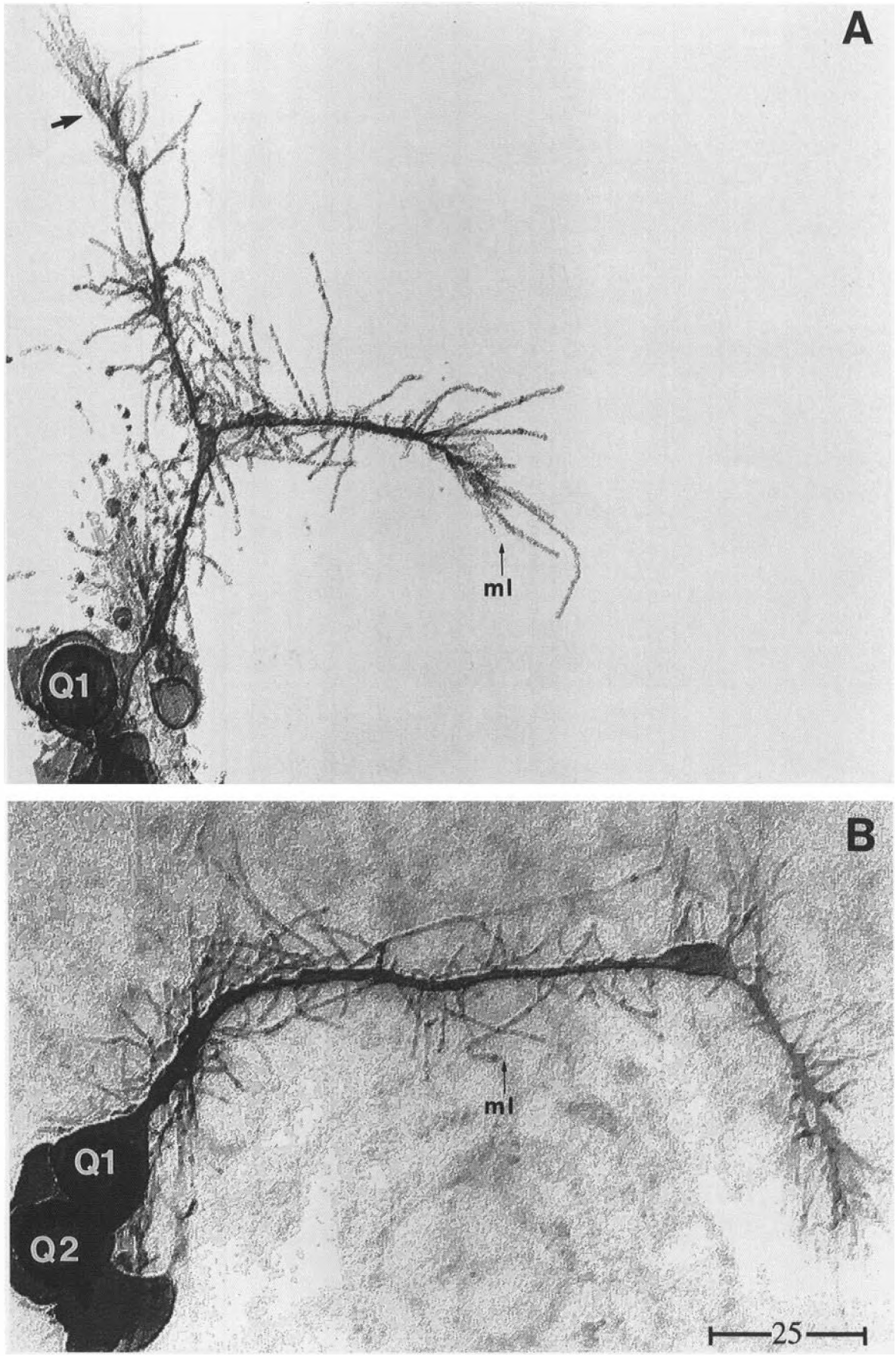
A
ml
Q1
B
ml
Q1
Q2
25

In the remaining seven observations of the Q1 growth cone at the midline, the growth cone did not halt but instead accelerated or maintained speed to cross the midline rapidly (Fig. 3, B). In three of these seven observations, we had labeled the Q1 neurons on both sides of the ganglion and could clearly determine that the acceleration occurred at the time filopodia of the pair of growth cones contacted each other (Fig. 4). The contacting filopodia thickened and were stabilized, persisting for up to 4 hr; in contrast, at 32% of development, the longest-lived filopodium endured for only 80 min. The growth cone advanced rapidly by flowing forward and filling the space between the stabilized filopodia, a process resembling the filopodial dilation described by O'Connor et al. (1990). After this rapid advance, however, all of the growth cones paused in their growth for 30–90 min at a point 5–15 μm beyond the midline (Fig. 3, A and B), and in two instances retracted to the midline.

Q1 interaction at the midline

The strong interaction between the growth cone of Q1 and the growth cone of its contralateral homolog suggests that this interaction could be significant in pathfinding. To test this hypothesis, one Q1 and Q2 were ablated in each of 41 ganglia before 32% of development (after axogenesis, but before the growth cone had begun to grow toward the midline). The embryos were then cultured for 24 hr and the growth of the surviving Q1 assayed. In 51% of the cases, the Q1 growth cone had stopped at the midline, failing to cross the midline in the absence of its contralateral homolog. In an additional 10% of the cases, Q1's growth cone had progressed along the appropriate path to the midline, but then mismigrated, either turning rostrally and extending along aberrant courses that varied from animal to animal, or sprouting secondary growth cones that grew along other pathways (Fig. 5). In the remaining 39%, the growth cone extended normally to the contralateral MP1/dMP2 pathway.

We also observed with time-lapse video microscopy three additional instances in which one Q1 was killed. In all three cases, the surviving Q1 extended a growth cone to the midline, where it stopped for 8 hr or more. The growth cone neither extended nor retracted during this period, although it remained active, extending filopodia in all directions, including across the midline. There was no apparent inhibition of filopodia crossing the midline; these filopodia reached lengths of 40 μm, and in two instances could contact the labeled processes of the dead contralateral Q1 (the distance from the midline to the MP1/dMP2 fascicle is approximately 45 μm). Although no filopodial stabilization was observed in either of these cases as was observed routinely in contacts between living Q1 growth cones, one of these growth cones did progress across the midline after a prolonged delay, almost reaching the contralateral MP1/dMP2 pathway before the experiment was terminated.

Filopodial activity

One striking result of the time-lapse observations is the dynamic activity of filopodia. Growth cones are surrounded by a number (20 ± 5 measurable) of radiating filopodia (Fig. 6) flickering in and out at rates of approximately 100 μm/hr (Table 1). The average filopodium has only a brief lifetime of approximately 35 min, ranging from 20 to 80 min. Almost none of the filopodia observed remain still for more than a few minutes, with a few noticeable exceptions to be described below. All either actively extend or retract, and many engage in repeated cycles of extension and retraction before finally withdrawing (Fig. 7).

Despite this vigorous activity, however, lateral movement of filopodia is minimal. Most, but not all, of the filopodia are relatively straight, and all movement is exclusively along a simple and unchanging linear track. We saw no instances of filopodial "oaring" or any translocation of the filopodial shaft (Bray and Chapman, 1985). Those filopodia that follow a curved or complex path (Figs. 6, 8) are generated by the extension of the tip along a complex path, not by any late deformation or buckling of initially straight filopodia. Any change in the trajectory of the filopodium is made at the tip, and the shaft of the filopodium remains rigidly in place, as if either its cytoskeletal elements are inflexible or it is adherent to the substrate along its length. During retraction, filopodial tips recapitulated their initial path in reverse. Filopodia that reextended usually repeated their original trajectory precisely, although in a few instances reextending filopodia projected in novel directions (Fig. 8).

We have attempted to make correlations between filopodial activity and growth cone behavior. At 32% of development, the Q1 growth cone is in the process of making a medial turn (Fig. 2, 4 hr); at 32.5%, the growth cone has completed the turn and is extending medially, toward the midline (Fig. 2, 8 hr). In Figures 9 and 10, we have plotted several parameters of filopodial behavior against filopodial orientation. One general morphological attribute of the Q1 growth cone as it turns medially is that the majority (82%) of its filopodia are also oriented medially. This asymmetry in filopodial distribution does not arise by selection of medially oriented filopodia; more filopodia are initiated from the medial side of the growth cone than from the lateral side (Figs. 9, 10). Furthermore, although medially oriented filopodia do tend to be longer and survive slightly longer than laterally oriented filopodia, the differences are not substantial enough to account for the difference in distribution. The rates of extension and retraction also show no significant bias with respect to their orientation. If filopodia were stabilized by contact with a preferred substrate located medially (as we have observed in some filopodia that cross the midline, in Figs. 4, 7), we would expect that the rate of medial extension would be

←

Figure 5. Ablation of the Q1 and Q2 neurons on one side of a ganglion results in abnormal pathfinding by the surviving Q1 after its growth cone reaches the midline. *A*, Q1 and Q2 were ablated on the right side of the third thoracic ganglion 24 hr before this picture was taken. The surviving Q1 grew normally to the midline, but failed to progress beyond it. Filopodia do extend across the midline, but all normal growth cone migration is stopped. This particular cell also extended an aberrant rostral axon (growth cone is marked with an *arrow*) that extended along the ipsilateral MP1/dMP2 pathway. This is the path along which Q1 often overshoots at 32% of development, prior to turning medially. This cell is a unique case, however; in the absence of its homolog, Q1 typically (51% of the time) simply stops at the midline (*ml*, marked with an *arrow*), with no other aberrant pathfinding. In another 10% of the cases, the Q1 growth cone begins "wandering," extending along no known pathway. *B*, A control segment (the second abdominal) in the same animal. If Q1 finds its contralateral homolog at the midline, it grows normally to the contralateral MP1/dMP2 pathway as in this case. There is a rostrocaudal gradient of development, so that the second abdominal segment is approximately 2% of development less advanced than the third thoracic segment. If the Q1 in panel *A* had grown normally, then, it should have extended about 80 μm farther than the Q1 in this segment.

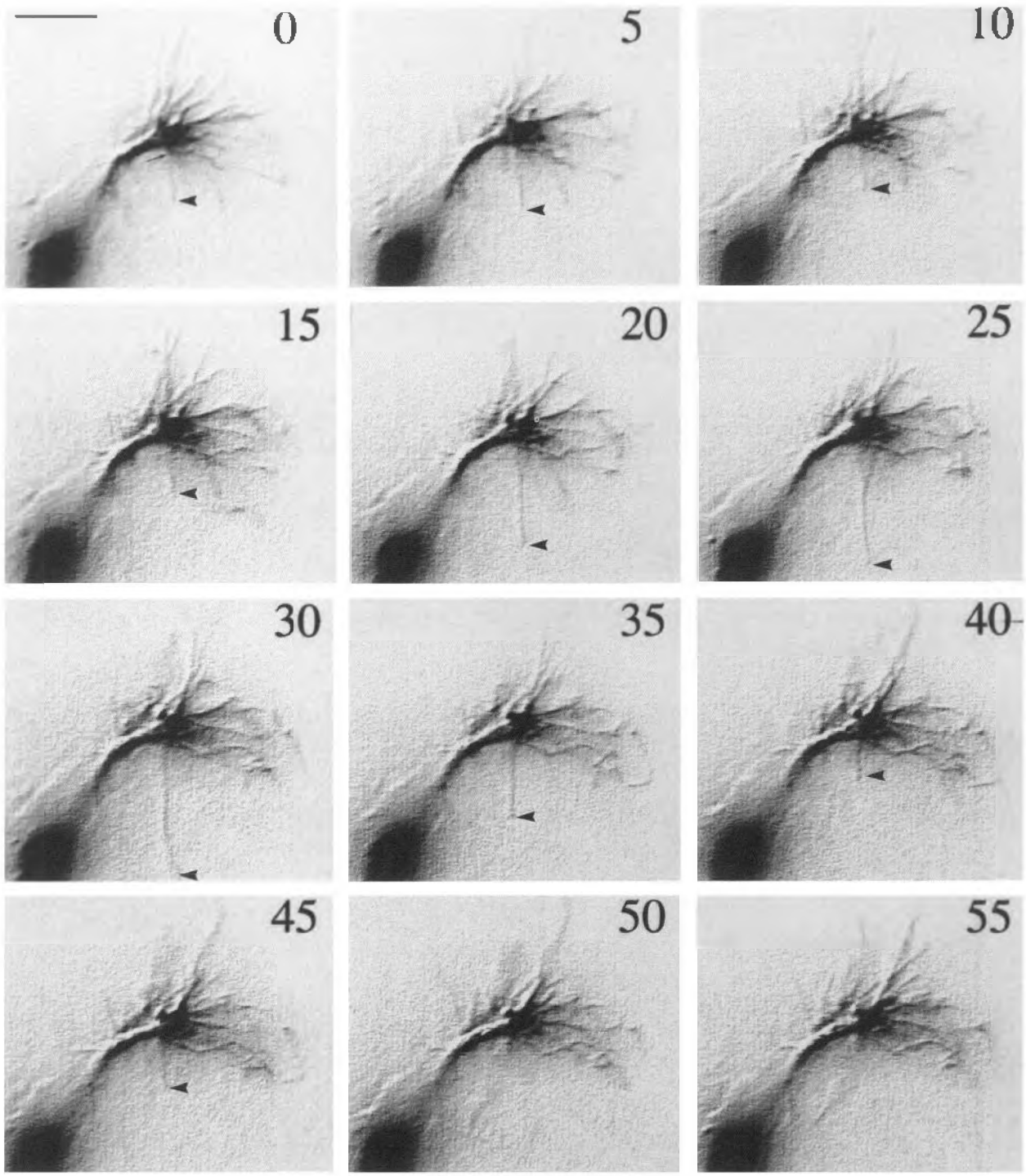

Figure 6. The growth cone is surrounded by an ; ctive corona of long filopodia. In this series of frames separated by 5 min intervals, most of the filopodia are relatively straight, but instances of ı arved and more complex shapes can be seen. In this and other fragments of time-lapse series illustrated in this article, edges have been artificiall enhanced with a shadowing convolution, and the fluorescent images have been digitally inverted to produce a dark, labeled neuron on a light bacl ground. Filopodial behavior was analyzed by tracking the length and orientation of individual filopodia frame by frame. In this example, an isolated filopodium can be seen extending caudally from the growth cone; its tip is marked in each frame by an *arrowhead*. For each frame, the length of the filopodium was measured by using a computer to trace it from the point it can first be distinguished from the mass of the growth cone (e.g., the *arrow* in frame 0) to the tip. The orientation is determined by a vector measured from the estimated center of the growth cone to the tip. Isolated filopodia such as this example are easy to measure. Other filopodia, for example the many filopodia extending medially (to the right in this figure), appear more ambiguous. However, the ability to integrate several frames visually by playing back short segments of the time-lapse, and the option to optimize images for maximum contrast without regard for esthetics, allows us to measure 20 ± 5 filopodia in each frame. Scale bar, 25 μm.

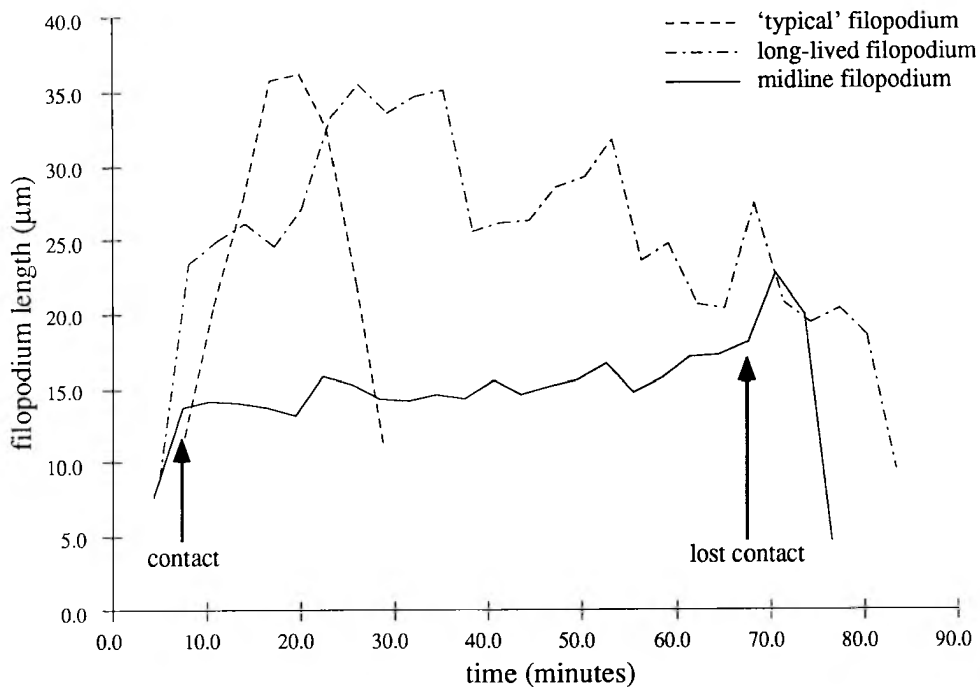

Figure 7. Individual filopodia have short but active lives. The lengths of 186 filopodia were measured at 3 min intervals, from the time they were first detectable to the time they had retracted and disappeared; the changing lengths of three representative filopodia over time are plotted here. Most filopodia behaved as plotted for the *typical filopodium.* They extend rapidly at 80–100 μm/hr to reach a length of 20 μm or more, and then retract equally rapidly, all within approximately 35 min. In this specific example, the filopodium survived for 30 min and its mean extension rate is somewhat greater than the average, at 122.0 μm/hr. Filopodia that survive for longer periods of time do not do so by growing to longer lengths, or by extending significantly more slowly. Instead, as shown for a representative *long-lived filopodium,* they undergo repeated cycles of extension and retraction. They also do not show any prolonged periods of stability. This particular example has several brief periods of little change in length that span a single sample point; these short "rests" probably represent an artifact of sampling, in which the peak or trough is missed in the data set. This artificial truncation means that any filopodium that extends and retracts multiple times will be more likely to exhibit these false "rests," and therefore have a reduced mean extension rate. This particular filopodium has a mean extension rate of 59.1 μm/hr. An exception to this absence of stability is plotted for a *midline filopodium.* In this instance, we had labeled the Q1 neurons on both sides of the midline with DiI; at the time labeled *contact,* this filopodium crossed the midline and its tip contacted the shaft of a labeled filopodium from the contralateral Q1. The two filopodia maintained contact for an hour, and although there was some back-and-forth movement, the filopodia remained at a relatively constant length and position over this entire time period. At the time labeled *lost contact,* the contralateral filopodium abruptly retracted, and the filopodium surged forward briefly before retracting equally abruptly. Note that the long stable periods in this filopodium extend over multiple samples, and are therefore unlikely to be an artifact of the sampling interval. This filopodium has a mean extension rate of 25.0 μm/hr.

noticeably lower than lateral extension rates; no such specific local variation could be detected.

As can be seen from Figures 9 and 10, more filopodia are extended in the direction of future growth, and those that extend along the path of outgrowth also tend to survive longer. There is no clear correlation of filopodium length with orientation. Long filopodia may be extended orthogonally to the path of outgrowth, but they do not persist and are rapidly retracted. Filopodia that do persist for longer periods of time do so chiefly because they go through more cycles of retraction and prompt reextension (Fig. 7).

A coarser analysis of the behavior of filopodia is illustrated in Figure 11. Filopodia were grouped into two classes, those that extend to any degree in the direction of outgrowth (in this case, medially) and those that extend away from the direction of outgrowth (laterally). This approach allows us to determine a simple bias score that quantifies the degree to which the parameter compares with the direction of growth cone extension. For example, the number of filopodia at 32% of development has a bias score of 4.8, indicating that 4.8 times as many filopodia extend medially as laterally. Although the number of filopodia is unambiguously skewed medially, none of the other parameters of filopodial behavior (duration, length, or rates of extension and retraction) have bias scores significantly different from 1 ($p > 0.1$), indicating a lack of measurable correlation with the direction of outgrowth.

Discussion

Growth cone migration

Previously, we had built up our ideas about the timing of growth cone migration from static images captured at relatively long intervals, and when viewed on a coarse time scale, growth cone movements give an impression of a steady progression. When viewed on the finer scale of our time-lapse studies, however, growth cones are actually seen to advance in a series of lurches, hesitations, and backtracking. For the most part, these impedimenta to the steady march of the growth cone appear to be random. No pattern to their distribution in time or space can be found in comparisons between similar growth cones in different animals. This observation should not be surprising, given that the growth cone possesses a wide array of filopodia that can flicker out to distances of 40 μm or more; with this reach, the growth cone can potentially contact half or more of the cells in the embryonic ganglion. The growth cone is therefore sampling a large proportion of a very complex environment, and aggregate growth might be expected to result from following

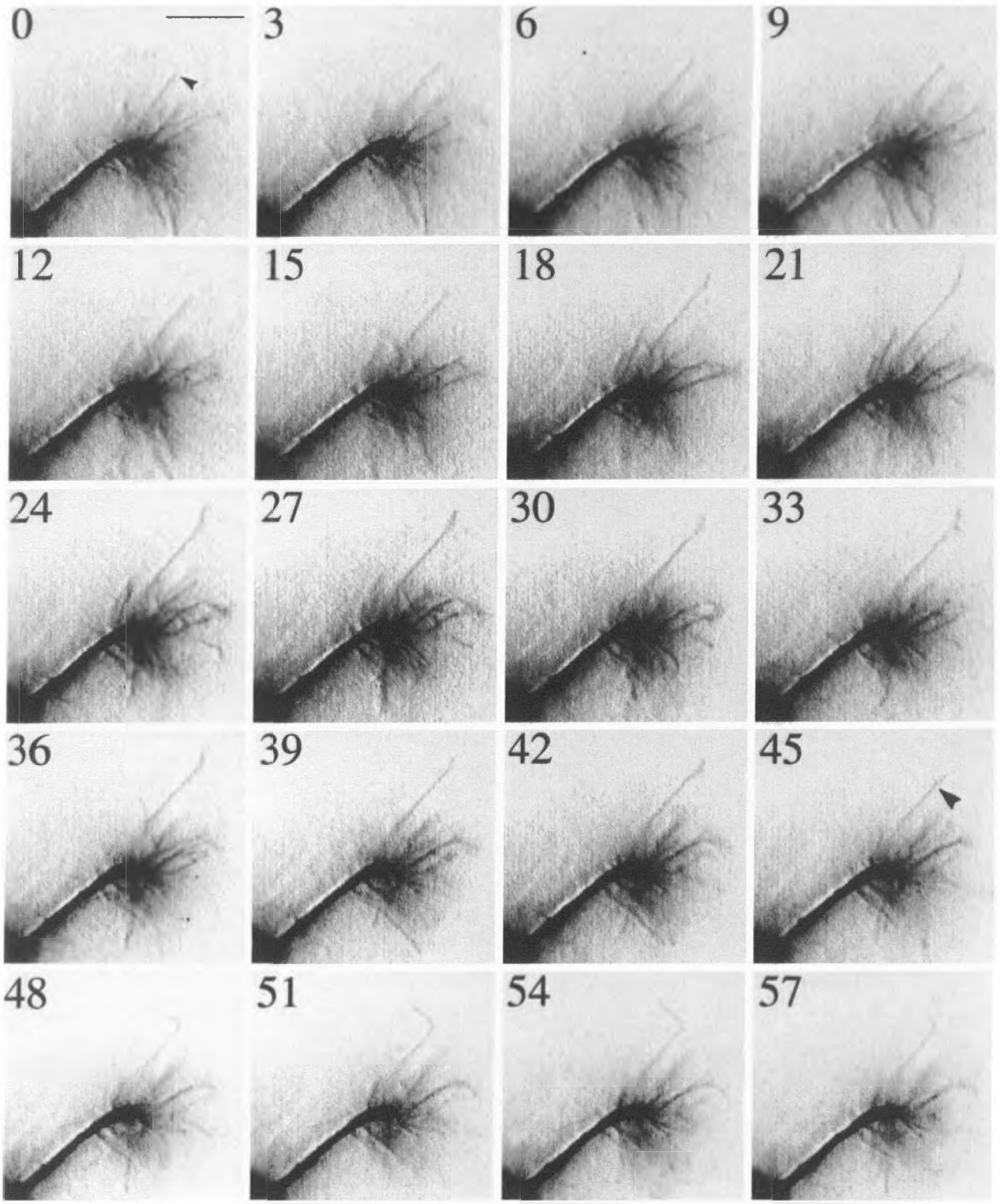

Figure 8. Although most filopodia are very straight, curved, bent, or, in this case, branching filopodia also can be found. The frames in this time series are 3 min apart, and cover the entire observed lifetime of the filopodium marked with an *arrowhead* at times *0* and *45* (hr). This filopodium was not visible in the frames immediately before and after this sequence; because it is quite long (10–15 μm) in the first and last frames, either its initial extension and final retraction were remarkably rapid, or the filopodium translocated from an out-of-focus plane into view. The Q1 growth cone is positioned directly over the unlabeled MP1 soma at this time. The indicated filopodium extends rostrally and medially, and at its greatest extent reaches within 15 μm of the midline. Unlike most filopodia we have observed, this one maintained a relatively stable length for an extended period of time (from time *18* to time *42* hr). After it began retracting, it first formed a small bud (*45, arrowhead*) that subsequently extended at right angles to the main axis of the filopodium (*48* and beyond). Scale bar, 25 μm.

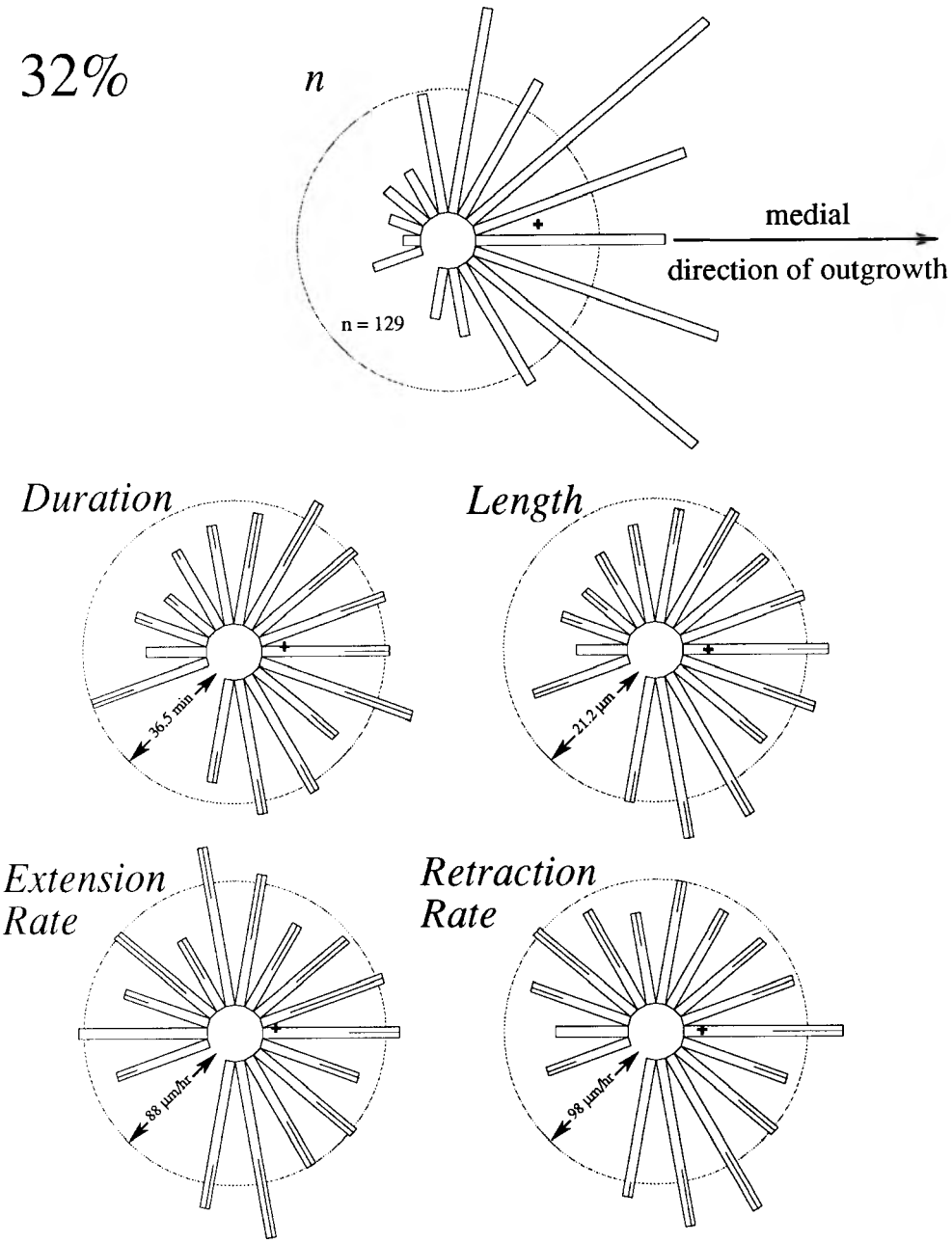

Figure 9. A radial plot of various parameters of filopodial behavior at 32% of development. The orientation of each *bar* represents the orientation of the filopodia, with medial to the right and rostral to the top. The *length* of the bar is a measure of the average value for each parameter; the *lines* at the end of each bar represent the SD, and the *circle* drawn in each graph represents the mean value. The *small cross* in each plot represents the end point of the mean vector (Table 1), normalized to the mean. A cross at the base of a bar would indicate that the vector sum of all the bars was 0; if all the filopodia were in a single bin, the vector sum would lie on the average *circle.* The data in this chart were collected from 129 filopodia and five growth cones. All five growth cones were at the choice point where they would cease growing rostrally and begin turning medially. The distribution of filopodia on Q1's growth cone is clearly asymmetric. Many more filopodia are initiated from the medial side of the growth cone than the lateral side. Individual filopodia, however, behave similarly no matter from which side of the growth cone they emerge. There is a small, statistically significant bias for medially oriented filopodia to be longer and survive for a greater period of time than laterally oriented filopodia, but this bias is not equivalent in scale to the bias in the distribution of numbers of filopodia, and is also not reflected in the rates of extension and retraction of filopodia. Medially oriented filopodia survive somewhat longer because they tend to go through more than one cycle of extension and retraction.

specific cues detected stochastically against a background of conflicting signals.

Against this variability, we have identified predictable patterns of behavior by the Q1 growth cone. At the first pathway choice Q1 must make, where it departs from its initial rostral growth to turn toward the midline, the growth cone consistently overshoots its final turning point and extends rostrally an additional 10–15 μm. The behavior suggests that the longitudinal cues Q1 first follows may extend at least a short distance farther rostrally, and that Q1 chooses between two alternative routes. The MP1 neuron also extends a short rostral branch at this same point, and the Q1 growth cone could respond to the same pathfinding cues that MP1 follows, or could simply retain its contact with the MP1/dMP2 fascicle for a short distance beyond its turning point. Another reproducible behavior by the Q1 growth cone poses a potential deciding factor in this choice: the soma of the MP1 neuron lies approximately 10 μm medially to this choice point, and the Q1 growth cone will attempt to increase its contact with the MP1 soma as it passes, by either flattening over its surface or making transient branches. The behavior indicates a strong adhesive interaction between Q1 and MP1 and, as filopodia from Q1 can easily reach the MP1 soma from the choice point, may lead the growth cone to its correct medial path.

One complication in this proposal is that Q1 must ultimately pass by the MP1 soma to grow toward the midline. Although there are distinctive morphological changes in the growth cone as it contacts the MP1 soma, there is no consistent concomitant delay in its progress; Q1 embraces MP1 en passant but continues relatively unchecked to the midline. The cues that lead Q1 to the midline are, at present, a mystery. The behavior of the Q1 growth cone at the midline indicates contact-mediated inhibi-

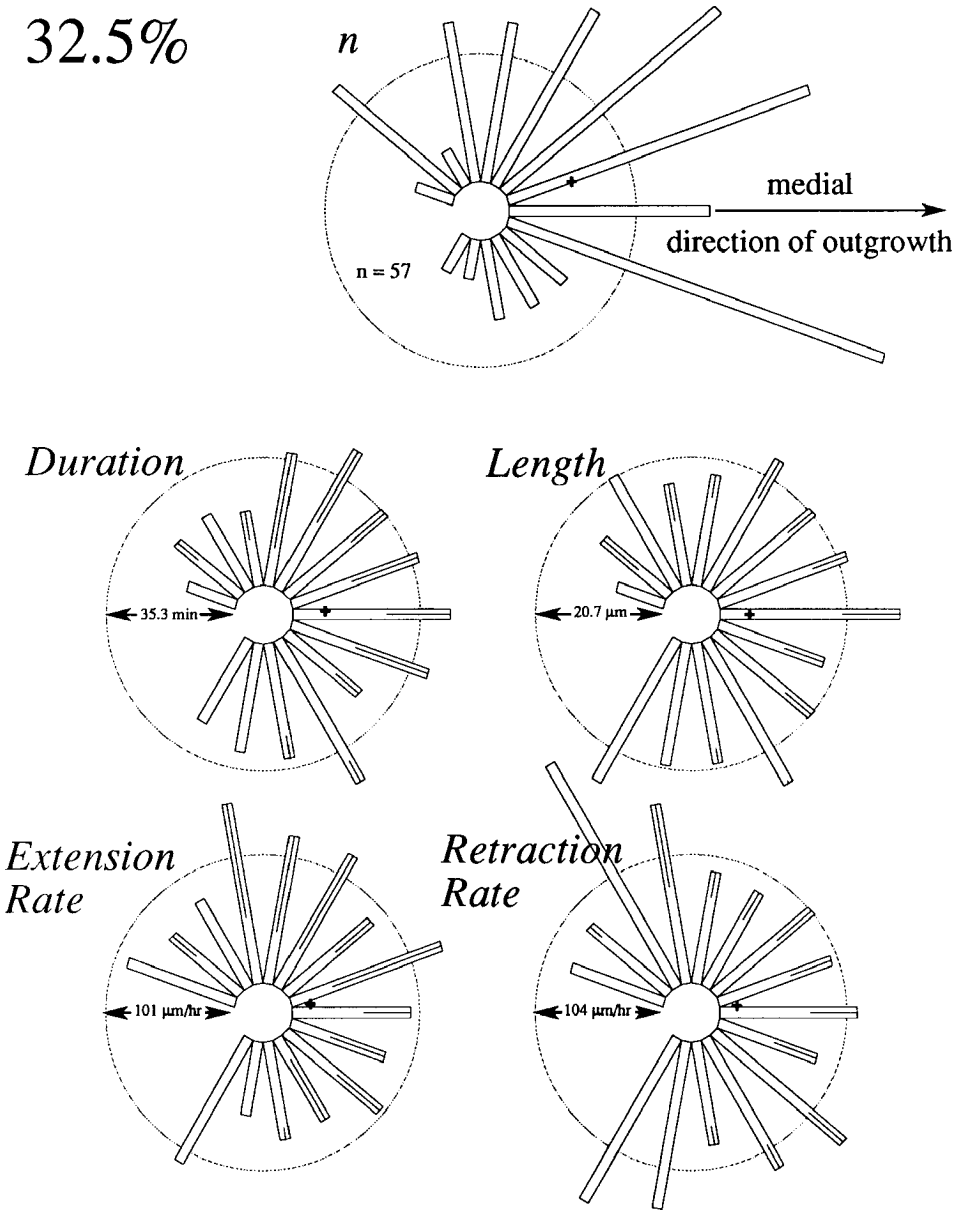

Figure 10. A radial plot of various parameters of filopodial behavior at 32.5% of development. The data in this chart were collected from measurements of 57 filopodia and three different growth cones. The parameters measured and the conventions used in this chart are identical with those used in Figure 9. The sole difference is the time the measurements were made; at this stage, all three growth cones had completed their medial turn and were growing steadily to the midline. As for growth cones at 32%, Q1 growth cones at 32.5% are markedly asymmetric, but the asymmetry is not strongly reflected in the behavior of individual filopodia. There is, however, a sharp change in the distribution of filopodia between 32% and 32.5%. At 32% (Fig. 9), there is a relatively numerous population of filopodia that extend caudally and medially from the growth cone; these filopodia extend over the corner cells. At 32.5%, the growth cone has advanced medially several micrometers, and the filopodia that would contact the corner cells would be extending directly caudally. Note that at this time point, this group of filopodia is greatly diminished, and there are relatively few filopodia extending over the corner cells. Again, however, there are no obvious correlates in the behavior of individual filopodia that could be causing this reduction. Filopodia to the corner cells at 32.5% of development are not significantly shorter lived than equivalent filopodia at 32%, for instance.

tion (Kapfhammer and Raper, 1987), not preferential adhesion with a guidepost cell. We presume that there must be some unidentified signal leading Q1 to the midline, and that some element at the midline, perhaps glial in nature (Klämbt et al., 1991), acts as a local inhibitory barrier. This barrier can be overcome by cooperative fasciculation between Q1 and its contralateral homolog (Fig. 4).

Cooperative fasciculation with the contralateral Q1 seems to be essential in allowing Q1 to cross the midline, as Q1 typically fails to cross the midline in the absence of its contralateral homolog (Fig. 5). Although a significant proportion (39%) of the Q1 growth cones were able to cross the midline after ablation of the contralateral Q1 and Q2 neurons, time-lapse observations revealed that filopodia from the surviving Q1 could reach remnants of the ablated cell in at least some instances, so the growth cones that advanced normally are most likely a consequence of the inadequacy of the ablation techniques used.

Our preceding observations (Myers and Bastiani, 1992) of Q1 outgrowth, using the more traditional methods of building an overview of development by taking a series of static images of the growth cone, revealed nothing unusual at the midline. Views of normal development with time-lapse microscopy and of development after ablating a specific component, the contralateral Q1 and Q2, have revealed a much more complex picture of commissure formation. Multiple cues must interact to guide Q1's growth cone across the midline. One unidentified factor must guide the growth cone in its growth from the ipsilateral MP1/dMP2 fascicle to the midline. The lack of any observable focal response by Q1's filopodia to any discrete guidepost in its environment suggests that this cue may be relatively diffuse, as might be generated by a diffusable factor (Placzek et al., 1988; Tessier-Lavigne et al., 1988) or a gradient fixed to the surfaces of cells or the basement membrane. A second unidentified factor is the midline element that blocks advance by the growth cone; we believe that midline glia or neuroepithelial cells are likely candidates for forming this barrier. By analogy with the vertebrate floorplate, it is possible that the midline structure is also the source for the cue that attracts the Q1 growth cone to the

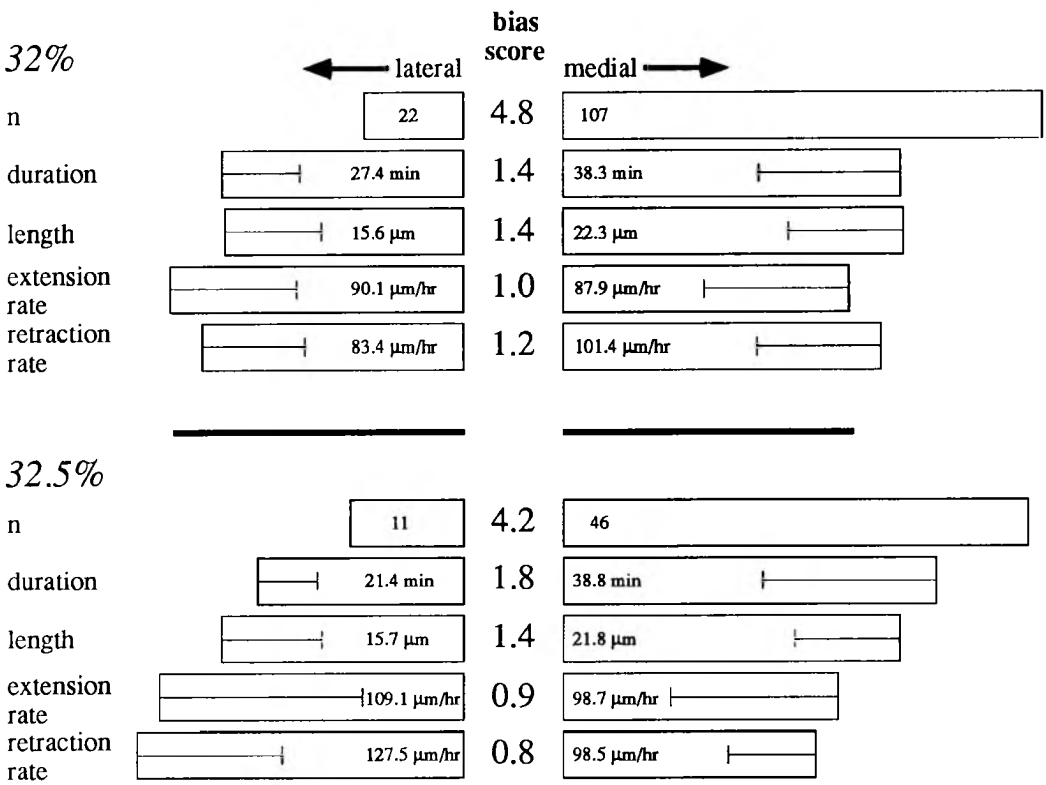

Figure 11. The data from Figures 9 and 10 are here replotted after being grouped into just two bins, medially vs. laterally oriented filopodia. A *bias score,* which is the medial value divided by the lateral value, has been calculated to quantify the degree of skewedness for each parameter. The numbers of filopodia are decisively asymmetric, with 4.8 (at 32%) and 4.2 (at 32.5%) times as many filopodia initiated on the medial side of the growth cone as the lateral side. When pooled in this manner, all other parameters, length, duration, and extension and retraction rates are not significantly different from 1 or, in other words, are approximately equivalent for the lateral versus medial side of the growth cone.

midline. If the Q1 growth cone follows a gradient that peaks at the midline, the growth cone's behavior at the midline may be a response to a transition in the gradient at that point. The third factor, and the only one that we have yet identified, is the cooperative fasciculation between the two Q1 growth cones at the midline.

The role of filopodia

A distinctive feature of neuronal growth cones in grasshopper embryos is their extensive filopodia, and we attempted to identify a possible function for these strikingly long and exuberant processes. The functions most frequently ascribed to filopodia in the literature are either as sensory structures or as tension-generating locomotor elements (Bray and Chapman, 1985), although the likely importance of the latter function has been diminished by the observation that growth cones can extend quite well in the cytochalasin-induced absence of filopodia (Marsh and Letourneau, 1984; Bentley and Toroian-Raymond, 1986). The distribution of filopodia has been used in previous work (Bastiani et al., 1984) as an indicator of substrate preferences without any knowledge of the dynamics of filopodial activity. Filopodia have been observed to have specific, preferential orientations in fixed preparations, and one mechanism that had been hypothesized is that filopodia that made contact with a particular preferred substrate would be stabilized and maintained for extended periods. The recent observations of O'Connor et al. (1990) suggest that in some instances filopodia could provide a path for the rapid translocation of the growth cone by the mechanism of filopodial dilation. Filopodia that have contacted a presumably preferred substrate can be stabilized and directly transformed into a growth cone by expansion of their surface membrane and an influx of cytoplasm. We have also observed this pattern of filopodial stabilization by some of Q1's filopodia as they contact filopodia of Q1's contralateral homolog at the midline. There are some differences between our results and those of O'Connor et al. (1990), however. Their observations were made in the periphery, and demonstrated strong, selective responses by growth cones migrating over ectoderm and basement membrane to discrete guidepost cells. We have found a similar selective stabilization by a growth cone in the neuron-rich environment of the CNS in response to a contact with filopodia of another specific growth cone (Fig. 4).

However, this midline interaction by some of Q1's filopodia is the only instance of a specific change in filopodial behavior prompted by contact with some element in the environment that we have been able to detect. In particular, we have looked for similar examples of filopodial stabilization or dilation at the time when Q1's growth cone makes a choice to turn medially. We expected that any spatial variation in adhesivity would be reflected in a corresponding variation in the rates of extension and retraction of individual filopodia. Although we see a marked asymmetry in the distribution of filopodia, we saw no significant variations in the behavior of individual filopodia that could be correlated with that asymmetry. The preponderance of medially oriented filopodia on the Q1 growth cone is *not* a consequence of selective stabilization of medially versus laterally oriented filopodia; in general, laterally oriented filopodia are of almost the same length, survive almost as long, and extend and retract

at approximately the same rate as medially oriented filopodia. Rather, the asymmetry is generated at the growth cone itself, by the selective initiation of new filopodia in the preferred orientation.

How does the growth cone determine the preferred orientation? One possibility is that there are slight variations in adhesivity that are detected by small spatial variations in the tension generated by filopodia, and that those subtle variations are amplified by a positive feedback loop at the growth cone. For instance, a slightly greater adhesivity medially than laterally might cause medially oriented filopodia to exert more tension on the growth cone; tension on the growth cone membrane could induce more filopodia in that direction that, in turn, would also exert tension. Our data indicate that the differences in adhesivity in the case of Q1's growth cone would have to be very small, to the point that the difference cannot be detected by variation in the behavior of individual filopodia, but perhaps a large number of filopodia can detect a statistically significant difference. Recent measurements of an inferred gradient across the surface of the vertebrate tectum suggests that growth cones can recognize a concentration difference of only 1% across the width of the growth cone (Baier and Bonhoeffer, 1992). One potential reason for the extraordinary exuberance of Q1's filopodial arbor is that the growth cone is sampling a small portion of its environment with each filopodium, and if that environment is either relatively homogeneous or very noisy, it must integrate a larger number of samples in order to detect a minute signal.

Alternatively, the growth cone may be detecting nonadhesive signals. Our studies of dye coupling (Myers and Bastiani, 1992) showed that gap junctions could be made from filopodia to other filopodia, growth cones, and cell bodies, and suggested that filopodia could be linked to cellular substrates via specialized junctions. Bentley et al. (1991) have also demonstrated that the intracellular concentration of small ions, such as calcium, can be detectably changed by the formation of gap junctions between a growth cone and other cells in its environment. Bastiani et al. (1984) found that filopodial contacts were associated with ultrastructural changes in target cells. The filopodia protruded deeply into the cells, and could induce coated pits and vesicles, suggesting that cells may communicate with one another by additional mechanisms. Filopodia may not act primarily as mechanical, tension-generating elements that adhere strongly to substrates in their environment; rather, their most important function may be as sensory or information-carrying structures that bind transiently to extracellular molecules, or that form short-lived junctions with other cells.

A significant inference from our observations, however, is that growth cones are not restricted to using a single simple mechanism for pathfinding. The Q1 growth cone recognizes and follows several different cues during its development. Its initial outgrowth is by fasciculation with the MP1/dMP2 fascicle. Q1 then leaves the fascicle to follow an unidentified cue that, by the behavior of the growth cone, appears to be relatively poorly localized and weak. At the midline, the growth cone exhibits a complex set of behaviors that suggest both an inhibition by unknown midline elements and a strong affinity for a discrete signal, the growth cone of its contralateral homolog. Finally, the Q1 growth cone again leaves a substrate, the axon of its homolog, for which it has demonstrated an active preference, and reselects the MP1/dMP2 fascicle. What we have found is that the formation of as simple a pathway as Q1's, growing in an environment as relatively simple as that of the embryonic grasshopper CNS, requires multiple interactions that may involve qualitatively different mechanisms.

References

Baier H, Bonhoeffer F (1992) Axon guidance by gradients of a target-derived component. Science 255:472–475.

Bastiani MJ, Raper JA, Goodman CS (1984) Pathfinding by neuronal growth cones in grasshopper embryos. III. Selective affinity of the G growth cone for the P cells within the A/P fascicle. J Neurosci 4:2311–2328.

Batschelet E (1981) Circular statistics in biology. New York: Academic.

Bentley D, Toroian-Raymond R (1986) Disoriented pathfinding by pioneer neurone growth cones deprived of filopodia by cytochalasin treatment. Nature 323:712–715.

Bentley D, Keshishian H, Shankland M, Toroian-Raymond A (1979) Quantitative staging of embryonic development of the grasshopper, *Schistocerca nitens*. J Embryol Exp Morphol 54:47–74.

Bentley D, Guthrie PB, Kater SB (1991) Calcium ion distribution in nascent pioneer axons and coupled preaxonogenesis neurons *in situ*. J Neurosci 11:1300–1308.

Bray D, Chapman K (1985) Analysis of microspike movements at the neuronal growth cone. J Neurosci 5:3204–3213.

Godement P, Salaun J, Mason CA (1990) Retinal axon pathfinding in the optic chiasm: divergence of crossed and uncrossed fibers. Neuron 5:173–186.

Hammarback JA, Palm SL, Furcht LT, Letourneau PC (1985) Guidance of neurite outgrowth by pathways of substratum-adsorbed laminin. J Neurosci Res 13:213–220.

Harris WA, Holt CE, Bonhoeffer F (1987) Retinal axons with and without their somata, growing to and arborizing on the tectum of *Xenopus* embryos: a time-lapse study of single fibres *in vivo*. Development 101:123–133.

Harrison RG (1907) Observations on the living developing nerve fiber. Anat Rec 1:116–118.

Heidemann SR, Lamoureux P, Buxbaum RE (1990) Growth cone behavior and production of traction force. J Cell Biol 111:1949–1957.

Honig M, Hume RI (1986) Fluorescent carbocyanine dyes allow living neurons of identified origin to be studied in long-term cultures. J Cell Biol 103:171–188.

Kapfhammer JP, Raper JA (1987) Collapse of growth cone structure on contact with specific neurites in culture. J Neurosci 7:201–212.

Klämbt C, Jacobs JR, Goodman CS (1991) The midline of the *Drosophila* central nervous system: a model for the genetic analysis of cell fate, cell migration, and growth cone guidance. Cell 64:801–815.

Letourneau PC (1979) Cell–substratum adhesion of neurite growth cones, and its role in neurite elongation. Exp Cell Res 124:127–138.

Mardia KV (1976) Linear–circular coefficients and rhythmometry. Biometrika 63:403–405.

Marsh L, Letourneau PC (1984) Growth of neurites without filopodial or lamellipodial activity in the presence of cytochalasin B. J Cell Biol 99:2041–2047.

Myers PZ, Bastiani MJ (1991) NeuroVideo: a program for capturing and processing time-lapse video. Comput Programs Methods Biomed 34:27–33.

Myers PZ, Bastiani MJ (1992) Cell–cell interactions during the migration of an identified commissural growth cone in the embryonic grasshopper. J Neurosci 13:115–126.

Myers PZ, Eisen JS, Westerfield M (1986) Development and axonal outgrowth of identified motoneurons in the zebrafish. J Neurosci 6: 2278–2289.

O'Connor TP, Duerr JS, Bentley D (1990) Pioneer growth cone steering decisions mediated by single filopodial contacts *in situ*. J Neurosci 10:3935–3946.

O'Rourke NA, Fraser SE (1989) Gradual appearance of a regulated retinotectal projection pattern in *Xenopus laevis*. Dev Biol 132:251–265.

Placzek M, Tessier-Lavigne M, Jessel TM, Dodd J (1988) Tissue specificity and properties of a floor plate–derived factor that influences commissural axon outgrowth. Soc Neurosci Abstr 14:595.

Ramón y Cajal S (1937) Recollections of my life (Horne E, trans). Philadelphia: The American Philosophical Society.

Raper JA, Kapfhammer JP (1990) The enrichment of a neuronal growth cone collapsing activity from the embryonic chick brain. Neuron 2:21–29.

Smith SJ (1988) Neuronal cytomechanics: the actin-based motility of growth cones. Science 242:708–714.

Speidel CC (1933) Studies of living nerves. II. Activities of amoeboid growth cones, sheath cells, and myelin segments, as revealed by prolonged observation of individual nerve fibers in frog tadpoles. Am J Anat 52:1–79.

Taghert PH, Bastiani MJ, Ho RK, Goodman CS (1982) Guidance of pioneer growth cones: filopodial contacts and coupling revealed with an antibody to Lucifer yellow. Dev Biol 94:391–399.

Terasaki M (1989) Fluorescent labeling of endoplasmic reticulum. Methods Cell Biol 29:125–135.

Tessier-Lavigne M, Placzek M, Lumsden AGS, Dodd J, Jessel TM (1988) Chemotropic guidance of developing axons in the mammalian central nervous system. Nature 336:775–778.

Zheng J, Lamoureux P, Santiago V, Dennerll T, Buxbaum RE, Heidemann SR (1991) Tensile regulation of axonal elongation and initiation. J Neurosci 11:1117–1125.